Persistent Collision Complexes in the Reaction of Silyl Ions with Ethylene[1]

W. N. Allen and F. W. Lampe*

Contribution from the Davey Laboratory, Department of Chemistry, The Pennsylvania State University, University Park, Pennsylvania 16802. *Received March 9, 1977*

Abstract: The reaction of SiH_3^+ with C_2H_4 has been studied in a tandem mass spectrometer at relative kinetic energies in the range of 0.47 to 2.4 eV and at C_2H_4 pressures in the range of $2-80 \times 10^{-4}$ Torr. At low relative kinetic energies persistent collision complexes $SiC_2H_7^+$ are directly observed, in the absence of collisional stabilization, some 2×10^{-5} s after formation. Collisional stabilization by C_2H_4 increases the yield of $SiC_2H_7^+$ so that at 80×10^{-4} Torr this ion accounts for ~80% of the observed products. The other observed products are $SiC_2H_5^+$, $SiCH_3^+$, and $SiC_2H_3^+$. Extrapolation of product yields to infinite pressure indicates that the collision complex accounts for ~90% of total reaction with the other 10% of reaction being due to a direct process forming $SiCH_3^+$. The experimental data yield absolute values for the lifetime of energy-rich collision complexes, for the unimolecular rate constants for decomposition of the complex to $SiC_2H_5^+$ and $SiCH_3^+$, and for the single-collision stabilization of $SiC_2H_7^{+*}$ by C_2H_4. The strong collision assumption breaks down at the higher relative kinetic energies and a value of 0.7–1.1 eV for the maximum energy transferred per collision from $SiC_2H_7^{+*}$ to C_2H_4 may be derived. RRKM calculations based on the chemically activated molecule being $CH_3CH_2SiH_2^+$ and in which angular momentum of reactants is conserved give order-of-magnitude agreement with experiment.

Introduction

A major result of the introduction of beam techniques to the study of ion–molecule reactions[2-6] has been the development of a distinction between mechanisms that involve "persistent intermediates" and those that are "direct". A persistent intermediate is understood to be a collision adduct of the reactants which persists as a single molecular entity for at least a few periods of rotation, i.e., has a lifetime of at least 10^{-12} s. In a direct mechanism the reaction products separate in a time less than a rotational period of the reactant adduct.

The involvement of persistent intermediates in numerous ion–molecule reactions has been detected in beam studies[2,7-15] by the observation of symmetry in the angular and velocity distributions of product ion intensities about the center of mass of the system. Despite the strong evidence afforded by observed symmetry of product angular and velocity distributions, the surest basis for concluding that a persistent intermediate is involved is to detect it directly along with its decomposition products. It is not surprising that such direct detection of collision adducts has been rare because most previous beam studies have dealt with systems of so few internal degrees of freedom that the lifetimes of the collision adducts were necessarily much shorter[16] than the instrumental transit times.

Several years ago it was reported[17] from this laboratory that a beam of SiH_3^+ ions reacted with C_2H_4 in a collision cell to form $SiC_2H_7^+$ intermediates which were registered directly at the detector of the apparatus after a transit time of some 10^{-5} s. Inasmuch as the C_2H_4 pressure in the collision chamber was low (i.e., 10^{-3} Torr) and the phenomenological cross section for detection of $SiC_2H_7^+$ was extremely sensitive to collision energy (i.e., becoming zero at a barycentric energy of 1.5 eV), it was concluded[17] that the $SiC_2H_7^+$ ions were being detected as unstabilized, and therefore energy-rich, collision adducts or complexes. Subsequently, the direct detection of several other persistent collision complexes in beam experiments[18-20] has been reported.

Our recent studies of persistent collision complexes in the reactions of Si^+, SiH^+, and SiH_3^+ ions with C_6H_6[19,20] have shown that at collision chamber pressures of 10^{-3} Torr some collisional stabilization of energy-rich collision complexes does occur. This fact, and the rather small phenomenological cross sections for $SiC_2H_7^+$ observed,[17] suggested the possibility that the $SiC_2H_7^+$ ions detected in the earlier study[17] were actually collision complexes that had been collisionally stabilized. A reinvestigation of the $SiH_3^+ + C_2H_4$ reaction was therefore deemed to be warranted and this paper is a report of our results.

Experimental Section

SiH_3^+ ions were formed from SiH_4 in an electron-impact ion source and reacted with C_2H_4 in the collision chamber of a tandem mass spectrometer. This apparatus, which has been described previously,[21] consists of two quadrupole mass filters mounted "in-line" and separated from each other by ion lenses and the collision chamber. It permits the injection of mass-selected ions, having kinetic energies variable down to about 1 eV, into the collision chamber that contains the neutral reactant molecule. Product ions scattered in the forward direction are collected with an acceptance angle of ~10° and mass-analyzed. Ion-intensity measurements are made with a Bendix 4700 continuous-dynode electron multiplier.

The pressure of ethylene in the collision chamber was measured with a CGS Barocel capacitance manometer. Measurements of ArD^+ formation in the reaction

$$Ar^+ + D_2 \rightarrow ArD^+ + D \qquad (1)$$

were carried out with Ar^+ ions of 1.3 eV kinetic energy. Comparison with the rate constant–ion energy data of (1) reported by Teloy and Gerlich[22] indicates that the pressure measurements are accurate to within 8%.

The energy of the ionizing electron beam in the ion source was 85 eV and the trap currents were in the range of 10–20 μA. The reactant ion beam entering the collision chamber was found by retarding-field measurements to have an energy spread (full width at half-maximum) of about 1 eV. Most of this rather large energy spread was found to be caused by the passage of the ions through the quadrupole mass filter.

Considerations of the mass spectrum of SiH_4 at 85 eV and the natural distribution of silicon isotopes indicate the isotopic composition of the *m/e* 31 ion beam to be: $^{28}SiH_3^+$ (93.8%), $^{29}SiH_2^+$ (5.7%), and $^{30}SiH^+$ (0.5%). Corrections for this isotopic composition of the beam and for the natural abundance of ^{13}C in the C_2H_4 target were applied to all ion currents, using the cross sections for the reactions of SiH_2^+ and SiH^+ reported earlier.[17] Thus all results refer to ^{28}Si and ^{12}C species.

In calculating fractional abundances of product ions it is assumed that all product ions of SiH_3^+–C_2H_4 collisions are collected with equal efficiency. However, with conditions used, some 60–65% of the ion-transit time from collision chamber to detector is spent in the second mass filter. This means that while all collision complexes ($SiC_2H_7^+$) are formed in the collision chamber, the majority of product ions formed by unimolecular dissociation of $SiC_2H_7^+$ (predominantly $SiC_2H_5^+$) originate in the mass filter. There will be some discrimi-

Table I. Dependence of Ion Intensity on Collision Energy at 5×10^{-4} Torr

		Multiplier current in A $\times 10^{14}$ at collision energy of				
m/e	Ion	0.47 eV	0.94 eV	1.4 eV	1.9 eV	2.4 eV
31	SiH_3^+	4.65×10^4	9.97×10^4	1.72×10^5	1.99×10^5	2.25×10^5
43	$SiCH_3^+$	21	22	30	39	60
55	$SiC_2H_3^+$	10	16	30	44	69
57	$SiC_2H_5^+$	58	101	158	170	167
59	$SiC_2H_7^+$	48	30	21	6	

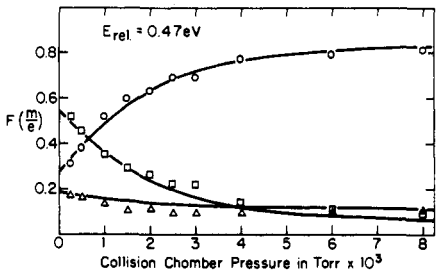

Figure 1. Ion fractions of total ionic product as a function of collision chamber pressure at a relative kinetic energy of 0.47 eV: O, $SiC_2H_7^+$; □, $SiC_2H_5^+$; △, $SiCH_3^+$.

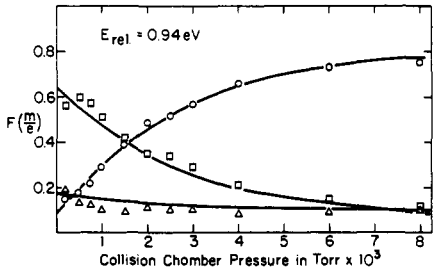

Figure 2. Ion fractions of total ionic product as a function of collision chamber pressure at a relative kinetic energy of 0.94 eV: O, $SiC_2H_7^+$; □, $SiC_2H_5^+$; △, $SiCH_3^+$.

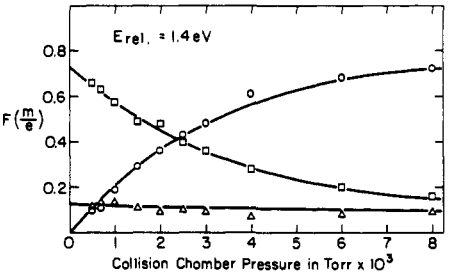

Figure 3. Ion fractions of total ionic product as a function of collision chamber pressure at a relative kinetic energy of 1.4 eV: O, $SiC_2H_7^+$; □, $SiC_2H_5^+$; △, $SiCH_3^+$.

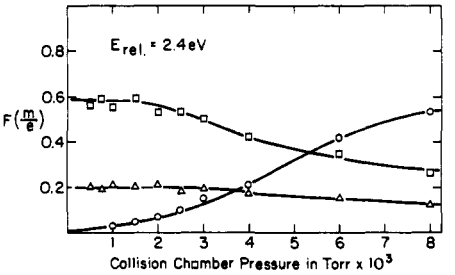

Figure 4. Ion fractions of total ionic product as a function of collision chamber pressure at a relative kinetic energy of 2.4 eV: O, $SiC_2H_7^+$; □, $SiC_2H_5^+$; △, $SiCH_3^+$.

nation against product ions that are formed in the filter and the extent of this discrimination will depend in a complicated manner on the location in the filter where the decomposition occurs, on the mass difference between parent and daughter ions, on the resolution being employed, and on the time spent in the filter. While we recognize the uncertainty that this discrimination imposes on our assumption of equal collection efficiency, we do not think the error involved is very serious for the following reasons: (1) Most of the product ions of the decomposition of $SiC_2H_7^+$ are $SiC_2H_5^+$ ions which differ by only two mass units from the parent. (2) We observe no differences in peak shape between $SiC_2H_7^+$ and $SiC_2H_5^+$ ions. (3) Comparison with earlier studies[17] from this laboratory on the same reaction, but in which the transit time through the mass filter was greater by a factor of 1.7–2.0, shows, within the precision of the data, no effect of quadrupole transit time on the fraction of $SiC_2H_5^+$ daughter ions. We could have definitely detected differences of 20% in this fraction between the two studies. Therefore we believe that the assumption of equal collection efficiencies is valid within an error of 20%.

SiH_4 was purchased from the J. T. Baker Chemical Co. It was subjected to several freeze–pump–thaw cycles and stored. Prior to use, it was checked mass spectrometrically for satisfactory purity. C_2H_4 was Phillips Research Grade and was used as received.

Results and Discussion

1. General Nature of the Reaction. When a beam of SiH_3^+ ions, having laboratory kinetic energies in the range of 1–5 eV, collides with C_2H_4 in a collision chamber at ambient temperature, the product ions observed are: $SiC_2H_7^+$ (*m/e* 59), $SiC_2H_5^+$ (*m/e* 57), $SiC_2H_3^+$ (*m/e* 55), and $SiCH_3^+$ (*m/e* 43).

The ion intensities observed at a collision chamber pressure of 5×10^{-4} Torr and for relative kinetic energies in the range of 0.47–2.4 eV are shown in Table I. The product ions observed and the phenomenological cross-sections obtained from the data in Table I are in accord with the earlier report.[17] Also in agreement with the earlier work is the fact, apparent from the data in Table I, that the cross section for observation of $SiC_2H_7^+$ (*m/e* 59) decreases extremely sharply with increasing collision energy. Up to a collision energy of 1.9 eV, the cross sections for the other three ionic products decrease with increasing energy as expected for exothermic reactions. Above 1.9 eV collision energy, the cross sections for the formation of $SiCH_3^+$ (*m/e* 43) and of $SiC_2H_3^+$ (*m/e* 55) increase with energy, suggesting the onset of endothermic reaction channels. The total cross section for formation of detectable products is a small fraction of the Langevin cross section for orbiting[23] and suggests that most of the $SiC_2H_7^+$ collision complexes revert back to reactants. The value of the ratio $\sigma_{Total}/\sigma_{Langevin}$ decreases from 0.16 at 0.47 eV to 0.11 at 0.94 eV. At higher energies, the Langevin cross section is not a meaningful concept.

At a constant collision energy, the relative yields of the products depend markedly on the pressure of C_2H_4 in the collision cell, as may be seen by reference to Figures 1–4. In these figures, the ion abundances, expressed as fractions of total ionic product, are plotted as a function of the pressure of C_2H_4. Generally, the abundance of $SiC_2H_7^+$ (*m/e* 59) increases with increasing pressure of C_2H_4 to apparent limiting values of the order of 0.8, while the abundances of $SiC_2H_5^+$ (*m/e* 57) and $SiCH_3^+$ (*m/e* 43) decrease with increasing pressure. The behavior of $SiC_2H_3^+$ is similar to that of $SiC_2H_5^+$ (*m/e* 57) but is not shown. The points in Figures 1–4 are the experimental

data obtained. The curves in Figures 1 and 2 are calculated using kinetic expressions derived in a subsequent section. The curves in Figures 3 and 4 are simply smooth curves drawn through the experimental points.

2. Kinetics and Mechanism. It may be seen in Figures 1 and 2 that at low collision energies the fractional abundance of $SiC_2H_7^+$ in the ionic reaction products does not become zero in the limit of zero pressure. However, the value of the finite limiting abundance does decrease with increasing energy. The intercept is indistinguishable from zero, at our sensitivity of detection, for relative kinetic energies of 1.4, 1.9, and 2.4 eV (the first and last of these being shown in Figures 3 and 4, respectively). These facts show that at the lower collision energies we are detecting $SiC_2H_7^+$ collision adducts that have not been stabilized by collision. However, at all pressures studied collisional stabilization is significant. For example, one may conclude from Figure 1 that at 0.47 eV relative kinetic energy and 10^{-3} Torr pressure of C_2H_4, the *m/e* 59 ion detected consists of 56% of $SiC_2H_7^{+*}$ (i.e., unstabilized) ions and 44% $SiC_2H_7^+$ (i.e., collisionally stabilized) ions. The ratio of pressure in the collision chamber to that of the vacuum housing surrounding it is such ($\sim 10^3$) that collisional stabilization must be occurring within the collision chamber.

Extrapolations of the fractional abundances of the other product ions to infinite pressure indicate that $SiCH_3^+$ reaches a high-pressure limiting abundance near 0.1 while $SiC_2H_3^+$ and $SiC_2H_5^+$ have high-pressure limiting abundances near zero. It is thus implied that the high-pressure limiting abundance of $SiC_2H_7^+$ should be near 0.9 and this is consistent with the data in Figures 1-3. We interpret this to mean that $SiC_2H_5^+$ and $SiC_2H_3^+$ arise predominantly by breakdown of $SiC_2H_7^{+*}$ but that $SiCH_3^+$ is formed partially by such breakdown and partially by a direct process not involving $SiC_2H_7^{+*}$.

The mechanism for the processes in our apparatus may therefore be written as in (2)-(7)

$$SiH_3^+ + C_2H_4 \xrightarrow{\sigma_c} SiC_2H_7^{+*} \quad (2)$$

$$SiH_3^+ + C_2H_4 \xrightarrow{\sigma_D} SiCH_3^+ + CH_4 \quad (3)$$

$$SiC_2H_7^{+*} + C_2H_4 \xrightarrow{k_s} SiC_2H_7^+ + C_2H_4 \quad (4)$$

$$SiC_2H_7^{+*} \xrightarrow{k_5(E^*)} SiC_2H_5^+ + H_2 \quad (5)$$

$$SiC_2H_7^{+*} \xrightarrow{k_6(E^*)} SiCH_3^+ + CH_4 \quad (6)$$

$$SiC_2H_7^{+*} \xrightarrow{k_7(E^*)} SiC_2H_3^+ + H_2 \quad (7)$$

It is not known whether $SiC_2H_3^+$ formation occurs by direct breakup of $SiC_2H_7^{+*}$, as shown by (7), or whether it is formed by further dissociation of $SiC_2H_5^+$. We have arbitrarily written the process as (7), but, whatever the actual mechanism, it can have no significant effect on our conclusions. Reaction 4 depicts collisional stabilization of the energy-rich collision adduct as a single-collision process occurring with a rate constant of k_s; this stabilization process represents the so-called strong-collision assumption.[16] Reaction 3 represents formation of $SiCH_3^+$ by a direct reaction independent of $SiC_2H_7^{+*}$ formation.

Reactions 2-4 can occur only in the collision chamber while reactions 5-7 may occur in the analyzer region of the tandem mass spectrometer as well as in the collision chamber. Therefore, we may write the following rate equations to describe the course of reaction *subsequent* to a collision that forms $SiC_2H_7^{+*}$

$$\frac{dI(SiC_2H_7^{+*})}{dt} = -(\tau^{-1} + k_s n)I(SiC_2H_7^{+*}) \quad \text{(collision chamber)} \quad (8a)$$

$$= -\tau^{-1}I(SiC_2H_7^{+*}) \quad \text{(analyzer region)} \quad (8b)$$

$$\frac{dI(SiC_2H_7^+)}{dt} = k_s n I(SiC_2H_7^{+*}) \quad \text{(collision chamber)} \quad (9)$$

$$\frac{dI(SiC_2H_5^+)}{dt} = k_5(E^*)I(SiC_2H_7^{+*}) \quad (10)$$

$$\frac{dI(SiCH_3^+)}{dt} = k_6(E^*)I(SiC_2H_7^{+*}) \quad (11)$$

$$\frac{dI(SiC_2H_3^+)}{dt} = k_7(E^*)I(SiC_2H_7^{+*}) \quad (12)$$

In (8)-(12), τ is the mean lifetime of $SiC_2H_7^{+*}$ with respect to unimolecular decomposition and is equal to $(\Sigma_j k_j(E^*))^{-1}$, n is the number density of C_2H_4 molecules in the collision chamber, and $I(SiC_jH_k^+)$ represents the ion current of the $SiC_jH_k^+$ ion.

Let t_c be the average time spent by $SiC_2H_7^+$ ions in the collision chamber and t be the average total time required for $SiC_2H_7^+$ to reach the exit of the analyzing quadrupole mass filter. The boundary conditions at $t = 0$ are

$$I(SiC_2H_7^{+*}) = \sigma_c n l I(SiH_3^+)$$

$$I(SiCH_3^+) = \sigma_D n l I(SiH_3^+)$$

$$I(SiC_2H_7^+) = I(SiC_2H_5^+) = I(SiC_2H_3^+) = 0$$

where l is the length of the collision chamber, and σ_c and σ_D are the cross sections for collision-complex formation and direct reaction, respectively. The integration of (8)-(12) is straightforward and it is convenient to express the integrated forms in terms of ion fractions of given *m/e* of total ionic product, i.e., $F(SiC_2H_7^{+*}) + F(SiC_2H_7^+) = F(59)$; $F(SiC_2H_5^+) = F(57)$; $F(SiC_2H_3^+ = F(55)$, and $F(SiCH_3^+) = F(43)$. Introduction of the total current of product ions, viz.

$$I(\text{product ions}) = (\sigma_c + \sigma_D)nlI(SiH_3^+) \quad (13)$$

leads to the integrated rate equations shown in (14)-(16).

$$F(59) = \left(\frac{\sigma_c}{\sigma_c + \sigma_D}\right) \times \left(\frac{k_s n + e^{-k_s t_c n}[\tau^{-1}e^{-t/\tau} + k_s n(e^{-t/\tau} - e^{-t_c/\tau})]}{\tau^{-1} + k_s n}\right) \quad (14)$$

$$F(57) = \left(\frac{\sigma_c}{\sigma_c + \sigma_D}\right) \times \left(\frac{k_5(E^*)[1 - \tau k_s n e^{-k_s t_c n}(e^{-t/\tau} - e^{-t_c/\tau}) - e^{-k_s t_c n}e^{-t/\tau}]}{\tau^{-1} + k_s n}\right) \quad (15)$$

$$F(43) = \left(\frac{\sigma_D}{\sigma_D + \sigma_c}\right) + \left(\frac{\sigma_c}{\sigma_D + \sigma_c}\right) \times \left(\frac{k_6(E^*)[1 - \tau k_s n e^{-k_s t_c n}(e^{-t/\tau} - e^{-t_c/\tau}) - e^{-k_s n t_c}e^{-t/\tau}]}{\tau^{-1} + k_s n}\right) \quad (16)$$

The expression for $F(55)$ is identical with (15) except that $k_5(E^*)$ would be replaced by $k_7(E^*)$.

Consideration of (16) for large n reveals that the ratio $\sigma_D/(\sigma_D + \sigma_c)$ may be obtained as the intercept of a plot of $F(43)$ vs. $1/n$. This then determines $\sigma_c/(\sigma_c + \sigma_D)$ since the sum of these ratios must be unity. In this way, it is found that at the

Table II. Experimental Lifetimes and Rate Constants

Collision energy, eV	$\tau \times 10^6$, s	$k_5(E^*) \times 10^{-5}$, s^{-1}	$k_6(E^*) \times 10^{-4}$, s^{-1}	$k_s \times 10^9$, cm^3/s
0.47	7.6 ± 1.6	1.1 ± 0.2	2.0 ± 0.4	2.5 ± 0.4
0.94	4.4 ± 1.9	2.0 ± 0.8	2.7 ± 1.2	3.3 ± 0.4

three lowest collision energies, 0.47-1.4 eV (Figures 1-3), the fraction of reaction proceeding through the complex $SiC_2H_7^{+*}$ is constant at 0.89 ± 0.01. The low-pressure limits of (14)-(16), which are the intercepts of Figures 1 and 2, are seen to be

$$\lim_{n\to 0} F(59) = \left(\frac{\sigma_c}{\sigma_c + \sigma_D}\right) e^{-t/\tau} \quad (17)$$

$$\lim_{n\to 0} F(57) = \left(\frac{\sigma_c}{\sigma_c + \sigma_D}\right) (1 - e^{-t/\tau})\tau k_5(E^*) \quad (18)$$

$$\lim_{n\to 0} F(43) = \left(\frac{\sigma_D}{\sigma_c + \sigma_D}\right) + \left(\frac{\sigma_c}{\sigma_c + \sigma_D}\right) (1 - e^{-t/\tau})\tau k_6(E^*) \quad (19)$$

with an expression for $F(55)$ that is analogous to (18). The intercepts of Figures 1 and 2 thus yield the fractional contributions of the observed product ions under collision-free conditions. However, as pointed out earlier, most of the collision complexes revert back to reactants in a dissociation reaction that is undetectable in our apparatus. To obtain the true lifetime of the complex, τ, and the unimolecular rate constants $k_j(E^*)$ it is necessary to correct the intercepts for the fraction of complexes decomposing back to reactants. This correction is made approximately by simply dividing the observed intercepts by the ratio $\sigma_{total}/\sigma_{Langevin}$. t is easily calculated from the known dimensions and potentials of the analyzer, and t_c, in the limit of zero pressure, is simply the time required for an ion of m/e 59 and known velocity to traverse one-half of the collision chamber. Therefore, from the corrected intercepts of Figures 1 and 2, absolute values of τ, the lifetime of $SiC_2H_7^{+*}$, and of the individual unimolecular rate constants, $k_j(E^*)$, may be calculated.

Given τ and $k_j(E^*)$, as well as relative values of σ_D and σ_c, one may determine absolute values of k_s by best fits of the data to (14)-(16). An approximate value of k_s may be obtained by estimating the initial slope of $F(59)$ vs. n since

$$\lim_{n\to 0} \left(\frac{dF(59)}{dn}\right) = \left(\frac{\sigma_c}{\sigma_c + \sigma_D}\right) k_s\tau \left(1 - e^{-t_c/\tau} - \frac{t_c}{\tau} e^{-t/\tau}\right) \quad (20)$$

In this way we have determined the experimental rate constants and lifetimes shown in Table II for relative kinetic energies of 0.47 and 0.94 eV. For the higher relative kinetic energies the intercepts could not be distinguished from zero, which means the average lifetime of unstabilized $SiC_2H_7^{+*}$ was too short for our detection sensitivity. In computing the curves of Figures 1 and 2, we have taken into account the pressure dependence of t_c by calculation of the average position in the collision cell of formation of $SiC_2H_7^{+*}$ as a function of the pressure of C_2H_4, using the Langevin cross section,[23] and by assuming, in addition, that those $SiC_2H_7^{+*}$ ions that make a collision with C_2H_4 have their velocity reduced to the velocity of the center-of-mass of the $SiC_2H_7^+ + C_2H_4$ system. The general validity of (14)-(16) and of the results in Table II is supported by the excellent agreement of the calculated curves with the experimental points in Figures 1 and 2.

It is interesting to note in Table II that the rate constant for stabilization is little changed when the relative kinetic energy is doubled from 0.47 to 0.94 eV. This is in accord with the "strong collision" assumption.[16] However, as may be seen in Figure 4, higher collison energies result in a very significant change of shape of the $F(m/e)$ vs. pressure curves. The expressions (14)-(16) which are based on the mechanism of (2)-(7) cannot account for the shapes of the curves in Figure 4. The most probable reason for the failure of (14)-(16) to account for the pressure dependencies of $F(m/e)$ in Figure 4 is the failure of the strong collision theory at higher energies. The shapes of the curves in Figure 4 suggest that at this collision energy (2.4 eV) two or more collisions of $SiC_2H_7^{+*}$ with C_2H_4 are required for stabilization. This departure from strong collision conditions was also observed at a relative kinetic energy of 1.9 eV and there is a suggestion of it beginning at 1.4 eV. As will be shown in a later section, the failure of strong collision conditions at a relative kinetic energy between 1.4 and 1.9 eV is in accord with the report that C_2H_4 can remove only up to 1.3 eV from internally excited cyclopropane on a single collision.[24]

3. Reaction Energetics and Potential Energy Profile. It is apparent from Figures 1-4 that the predominant reaction of SiH_3^+ at all energies studied is to form $SiC_2H_7^+$ and $SiC_2H_5^+$. The relative amounts of these two products, some 2×10^{-5} s after the reactant collision, depend on the extent of collisional stabilization. Previous high-pressure mass spectrometric studies[17] showed that as the pressure of C_2H_4 is increased considerably above the highest pressure of this study, the adduct $SiC_2H_7^+$, or equivalently, $SiH_3(C_2H_4)^+$, is replaced first by $SiH_3(C_2H_4)_2^+$ and then by $SiH_3(C_2H_4)_3^+$, but an adduct containing four C_2H_4 molecules is not observed. In addition, the pressure-dependent mass spectra were characteristic of what one would expect from $C_2H_5SiH_2^+$, $(C_2H_5)_2SiH^+$, and $(C_2H_5)_3Si^+$ ions. For these reasons, we believe the collision complex $SiC_2H_7^+$ observed in our beam studies to be ethylsilyl ion, $C_2H_5SiH_2^+$. Further, our experience with the mass spectra of alkyl silanes leads us to the conclusion that the most energetically favorable process eliminating H_2 from this ion (i.e., reaction 5) would form $CH_2{=}{=}CHSiH_2^+$.

The standard enthalpies of formation of $C_2H_5SiH_2^+$ and $C_2H_3SiH_2^+$ have not been measured. However, a reasonable estimate of $\Delta H_f^\circ(C_2H_5SiH_2^+) = 9.15$ eV may be made from the measured value of $\Delta H_f^\circ(CH_3SiH_2^+)$[25] and the establishment of a CH_2 increment of −0.16 ± 0.01 eV from comparisons of ΔH_f° values for a number of ethyl and methyl silanes as well as triethyl- and trimethysilyl ions.[25] Bond-energy considerations[26,27] then permit an estimate of $\Delta H_f^\circ(C_2H_3SiH_2^+) = 10.5$ eV. Using these values, the reaction of SiH_3^+ with C_2H_4 to form $C_2H_3SiH_2^+$ and H_2 is calculated to be exothermic,[25,27] as is also indicated experimentally by the dependence of the cross section on kinetic energy. The formation of the minor product $SiCH_3^+$ from ground-state reactants is endothermic by about 0.3 eV[28] and the dependence of the cross-section for formation of $SiCH_3^+$ on kinetic energy is consistent with this expectation if the SiH_3^+ contains small quantities of internally excited ions which can form $SiCH_3^+$ exothermically.

As mentioned earlier, the majority of orbiting encounters[23] between SiH_3^+ and C_2H_4 appear to revert back to reactants. Our interpretation of this is that there is a potential barrier which prevents a large majority of initial collision complexes, $SiH_3CH_2CH_2^{+*}$, from isomerizing to the more stable form $CH_3CH_2SiH_2^{+*}$. Most of the $SiH_3CH_2CH_2^{+*}$ ions dissociate

Table III. Vibrational Frequencies for Decomposition of $CH_3CH_2SiH_2^+$

Type of vibration	$\bar{\nu}$, cm^{-1}		
		Transition states	
	$CH_3CH_2SiH_2^{+*}$	II	I
C-H stretch	2946 (5)	2946 (4)	2946 (4)
Si-H stretch	2164 (2)	2164 (2)	2164 (2)
C-H bending	1392 (5)	1392 (5)	1392 (5)
Si-H bending	935	935	935
CH_3 rock.	979 (2)	979 (2)	979 (2)
SiH_2 rock.	570 (2)	570 (2)	570 (2)
CH_2 rock.	974 (2)	974 (2)	974 (2)
C-C stretch	1026	1539	1026
C-Si stretch	698	698	698
C-C-Si bend	239	239	239
CH_3 torsion	170	170	170
SiH_3 torsion	140	140	140

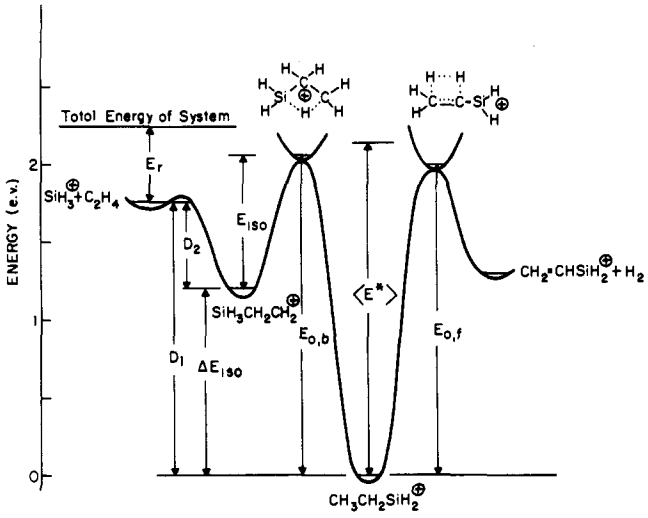

Figure 5. Potential energy profile along reaction coordinate. (Symbols are described in text.)

rapidly back to reactants but a small fraction isomerizes to $CH_3CH_2SiH_2^{+*}$. The latter ion and its dissociation products are the product ions detected. Since the total observed cross section decreases with collision energy somewhat faster than does the Langevin cross section, it would appear that the isomerization barrier separating $SiH_3CH_2CH_2^+$ from $CH_3CH_2SiH_2^+$ is slightly higher than the barrier separating $CH_3CH_2SiH_2^+$ from the reaction products (predominantly $CH_2{=}CHSiH_2^+ + H_2$). The use of bond dissociation energies[25,27] and vertical ionization potential data for R-SiH_2[25] and R-CH_2[29] radicals indicate the isomerization of $SiH_3CH_2CH_2^+$ to $C_2H_5SiH_2^+$ to be exothermic by 1.2 eV.

The considerations described above are consistent with the detailed mechanism shown in (2a,b) and (4′)-(6′), viz.

$$SiH_3^+ + C_2H_4 \rightleftarrows SiH_3CH_2CH_2^{+*} \quad (2a)$$

$$SiH_3CH_2CH_2^{+*} \rightleftarrows CH_3CH_2SiH_2^{+*} \quad (2b)$$

$$CH_3CH_2SiH_2^{+*} + C_2H_4 \rightarrow CH_3CH_2SiH_2^+ + C_2H_4 \quad (4')$$

$$CH_3CH_2SiH_2^{+*} \rightarrow CH_2{=}CHSiH_2^+ + H_2 \quad (5')$$

$$CH_3CH_2SiH_2^{+*} \rightarrow SiCH_3^+ + CH_4 \quad (6')$$

and with the potential energy profile shown in Figure 5. The heights of the energy barriers in Figure 5 were determined by unimolecular rate calculations as described in the next section.

4. Theoretical Rates of Collision Complex Decomposition. The rates of decomposition of $CH_3CH_2SiH_2^{+*}$ ions by the unimolecular processes (5′) and the reverse of (2b) have been calculated as a function of relative kinetic energy of reactants by the familiar Rice-Ramsberger-Kassel-Marcus (RRKM) expression[16]

$$k(E_v^*) = \frac{L^{\ddagger} \sum_{E_v^*-E_0} P(E_v^* - E_0)}{hN(E_v^*)} \quad (21)$$

In this expression, h is Planck's constant; $L^{\ddagger}$ is the number of kinetically equivalent paths; E^* is the total nonfixed internal energy of the $CH_3CH_2SiH_2^+$ ion, i.e., the internal energy that can "flow" between the various internal modes; $P(E_v^* - E_0)$ is the number of vibrational states of the activated complex that have energy equal to or less than $E_v^* - E_0$; $N(E_v^*)$ is the energy density of vibrational states of the energy-rich ion $CH_3CH_2SiH_2^{+*}$; and E_0 is the activation energy for the reaction. The relationship between the various energy parameters may be seen in the potential energy diagram shown in Figure 5. Rotational energy levels are not considered in the calculations, an omission which is warranted in view of the uncertainties in the thermochemistry and vibrational frequencies of the system.

The vibrational frequencies of the $CH_3CH_2SiH_2^+$ ion were assumed to be the same as those reported by Mackey and Watt[30] for the $CH_3CH_2SiH_3$ molecule, with the appropriate modes for one H atom bonded to the Si atom being removed. Frequencies of a given type of mode were grouped at the geometric mean of the individual values and these are shown in Table III. The transition states for isomerization back to $SiH_3CH_2CH_2^+$ (then to reactants) and for dissociation to the major products $CH_2{=}CHSiH_2^+ + H_2$ are shown respectively as I and II. In both transition states the reaction coordinate is

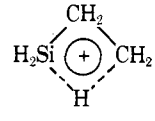

I

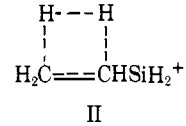

II

taken as a C-H stretching motion. The frequency of the C-C stretching motion was increased in transition state II to a value 50% higher than that of $C_2H_5SiH_2^+$. This is in accord with the report by Hassler and Setser[31] that in the four-center elimination of HCl from C_2H_5Cl, the carbon-carbon bond-order in the transition state is 1.8. It is also in accord with the type transition state used by Vestal[32] in calculations of the rate of unimolecular elimination of H_2 from $C_3H_8^+$ ions. All other frequencies were left unchanged from their values in $C_2H_5SiH_3$.[30]

The quantity E_v^* represents internal energy that is available for statistical flow among the vibrational modes. In view of the high angular momentum associated with ion–molecule reactions in particular, and with beam studies in general, not all

of the internal energy is available for flow through the vibrational modes of $SiH_3CH_2CH_2^{+*}$ and $CH_3CH_2SiH_2^{+*}$. A significant portion of it is locked into rotation to conserve the angular momentum of the system.

To take this into account approximately, consider the C–C–Si skeleton of the initial $SiH_3CH_2CH_2^+$ ion to be a linear species. Let the corresponding moment of inertia, I, define a single equilibrium distance, r_e, in the collision complex between an initial SiH_3^+ ion and C_2H_4 molecule by the relationship: $\mu r_e^2 = I$, where μ is the reduced mass of the reactants. The relationship between the kinetic energy of reactants in the center-of-mass system, E_r, and the total angular momentum, L, is as shown in (22),

$$E_r = \frac{L^2}{2\mu b^2} \tag{22}$$

where b is the impact parameter. The rotational energy of the assumed linear complex necessary to conserve angular momentum is

$$E_{rot} = \frac{L^2}{2\mu r_e^2} = \left(\frac{b^2}{r_e^2}\right) E_r \tag{23}$$

and this energy is not available for flow through the vibrational modes. The nonfixed energy of $SiH_3CH_2CH_2^{+*}$ is then a function of the impact parameter and is given by

$$E^*(b) = D_2 + E_r\left(1 - \frac{b^2}{r_e^2}\right) \tag{24}$$

where D_2 is the exothermicity of formation of $SiH_3CH_2CH_2^+$ (cf. Figure 5). The fraction of $SiH_3CH_2CH_2^{+*}$ ions that can surmount the isomerization barrier is the fraction whose angular momentum is sufficiently low that the nonfixed energy is equal to or greater than E_{iso}. Taking the barrier E_{iso} as a lower limit to $E^*(b)$ then leads to a critical impact parameter b_c, above which isomerization of $SiH_3CH_2CH_2^+$ cannot occur. This critical impact parameter is given by

$$b_c^2 = r_e^2\left(1 + \frac{D_2 - E_{iso}}{E_r}\right) \tag{25}$$

Similarly, the maximum impact parameter for complex formation can be obtained by the condition that $E^*(b) \geq 0$ and is given by

$$b_m^2 = r_e^2\left(1 + \frac{D_2}{E_r}\right) \tag{26}$$

The fraction of $SiH_3CH_2CH_2^{+*}$ that can isomerize is then

$$f_{iso} = \frac{b_c^2}{b_m^2} = 1 - \frac{E_{iso}}{D_2 + E_r} \tag{27}$$

and, since we believe the long-lived collision complexes in our experiments are $CH_3CH_2SiH_2^{+*}$, we assume, for simplicity, that all $SiH_3CH_2CH_2^+$ ions that can isomerize do so.

The average, nonfixed energy of the $SiH_3CH_2CH_2^{+*}$ ions that isomerize is

$$\langle E^*\rangle_{iso} = \frac{\int_0^{b_c} E^*(b)2\pi b\, db}{\int_0^{b_c} 2\pi b\, db} = \frac{1}{2}(D_2 + E_{iso} + E_r) \tag{28}$$

Assuming no change in moment of inertia on isomerization, we obtain finally the average, nonfixed energy of the $CH_3CH_2SiH_2^{+*}$ ions simply by adding the energy of isomerization, $D_1 - D_2$, to $\langle E^*_{iso}\rangle$. In terms of the barrier for isomerization back to $SiH_3CH_2CH_2^+$ (cf. Figure 5), the average nonfixed energy of $CH_3CH_2SiH_2^{+*}$ is then

$$\langle E^*\rangle = \frac{1}{2}(E_{0,b} + D_1 + E_r) \tag{29}$$

Table IV. Comparison of Calculated and Observed Lifetimes of $CH_3CH_2SiH_2^*$

	Relative kinetic energy of reactants	
	0.47 eV	0.94 eV
τ_{calcd}, μs	23.6	0.86
τ_{obsd}, μs	7.6 ± 1.6	4.4 ± 1.9

Using $\langle E^*\rangle$ from (29) (and Figure 5) along with the frequencies in Table III, unimolecular rate constants $k_j(E^*)$ were calculated as a function of collision energy E_r for (5′) and the reverse of (2b). The calculations were made using (21) and the Whitten–Rabinovitch approximation.[33] Calculations of the rate constant of (6′) were not carried out, since the thermochemistry is very uncertain and this reaction amounts to only about 10% or less of the decomposition of $CH_3CH_2SiH_2^{+*}$ at all kinetic energies studied. Appropriate corrections for the occurrence of (6′) were made from the experimental data in converting the unimolecular rate constants to lifetime of $CH_3CH_2SiH_2^{+*}$ by the relationship:

$$\tau = \left(\sum_j k_j(E^*)\right)^{-1}$$

The activation barrier for the forward reaction $E_{0,f}$ was taken to be 2.00 eV on the basis that the mean experimental activation energy reported by Robinson and Holbrook[34] for four-center H_2 elimination reactions is 2.0 ± 0.2 eV. This value is also in accord with the activation energy of 1.97 eV found by Davidson, Jones, and Pett[35] for the four-center HCl elimination from $CH_3CHClSiCl(C_2H_5)_2$. The activation barrier for the back reaction of $CH_3CH_2SiH_2^{+*}$ was taken to be at least equal to $E_{0,f}$ and the final value of 2.05 eV was arrived at to account for the ratio of $(\sigma_{product}/\sigma_{Langevin})$ observed at 0.47 eV, at which energy the Langevin treatment should be valid. The potential energy profile in Figure 5 depicts the various energy parameters for the specific case of E_r = 0.47 eV.

For comparison with experiment, these microscopic lifetimes must be averaged over the kinetic energy distribution of the reactant ion beam. The averaging was carried out graphically using a Gaussian kinetic energy distribution having a width at half-height of 1 eV in the laboratory frame of reference.

The calculated average lifetimes are shown in Table IV where they are compared with the experimental values found. The agreement, although only semiquantitative, is satisfactory, considering the uncertainties in the thermochemistry of the system, in the crude approximation of equating the vibrational frequencies of the $CH_3CH_2SiH_2^+$ to those of the $CH_3CH_2SiH_3$ molecule, and in the wide energy spread of the ion beam. This agreement attests to the general validity of the treatment and energy profile for the reaction shown in Figure 5. Clearly, further experiments, with ion beams of narrower energy spread to permit exploration of the relative kinetic energy region between 0.4 and 0.9 eV, are desirable.

It was pointed out earlier that strong collision conditions appear to fail at relative kinetic energies above 1.4–1.9 eV. According to (29), this means that the strong collision assumption fails when the average energy that must be removed from $CH_3CH_2SiH_2^{+*}$ to stabilize it exceeds 0.6–0.9 eV. Therefore, the maximum energy that can be transferred from $CH_3CH_2SiH_2^{+*}$ to C_2H_4 per collision is 0.6 to 0.9 eV. This conclusion is in agreement with the report by Setser, Rabinovitch, and Simons[24] that C_4H_4 can remove up to 1.3 eV per collision from chemically activated cyclopropane.

Acknowledgment. This work was supported by the U.S. Energy Research and Development Administration under Contract NO. EY-76-S-02-3416. Thanks are due to the Ed-

ucation Committee of the Gulf Oil Corporation for a grant that assisted in the construction of the tandem mass spectrometer. We also wish to thank Dr. Thomas M. Mayer for valuable comments and suggestions.

References and Notes

(1) U.S. Energy Research and Development Administration No. EY-76-S-02-3416-3.
(2) A. Henglein, K. Lacmann, and G. Jacobs, *Ber. Bunsenges. Phys. Chem.*, **69**, 279 (1965).
(3) R. L. Champion, L. D. Doverspike, and T. L. Bailey, *J. Chem. Phys.*, **45**, 4377 (1966).
(4) W. R. Gentry, E. A., Gislason, Y-T. Lee, B. H. Mahan, and C-W. Tsao, *Discuss. Faraday Soc.*, **44**, 137 (1967).
(5) Z. Herman, J. D. Kerstetter, T. L. Rose and R. Wolfgang, *Discuss. Faraday Soc.*, **44**, 123 (1967).
(6) A. Ding, A. Henglein, and K. Lacmann, *Z. Naturforsch.*, **23a**, 779 (1968).
(7) L. Matus, I. Opauczky, D. Hyatt, A. J. Mason, K. Birkinshaw, and M. J. Henchman, *Discuss. Faraday Soc.*, **44**, 146 (1967).
(8) L. D. Doverspike and R. L. Champion, *J. Chem. Phys.*, **46**, 4718 (1967).
(9) J. Durup and M. Durup, *J. Chim. Phys.*, **64**, 386 (1967).
(10) Z. Herman, A. Lee, and R. Wolfgang, *J. Chem. Phys.*, **51**, 452 (1969).
(11) A. Ding, *Z. Naturforsch.*, **24a**, 856 (1969).
(12) M. H. Chiang, E. A. Gislason, B. H. Mahan, C. W. Tsao, and A. S. Werner, *J. Phys. Chem.*, **75**, 1426 (1971).
(13) G. Eisele, A. Henglein, and G. Bosse, *Ber. Bunsenges. Phys. Chem.*, **76**, 140 (1974).
(14) G. Eisele and A. Henglein, *Int. J. Rad. Phys. Chem.* **7**, 293 (1975).
(15) G. Eisele, A. Henglein, P. Botschwina, and W. Meyer, *Ber. Bunsenges. Phys. Chem.*, **78**, 1090 (1974).
(16) P. J. Robinson and K. A. Holbrook, "Unimolecular Reactions", Wiley-Interscience, New York, N.Y., 1972.
(17) T. M. Mayer and F. W. Lampe, *J. Phys. Chem.*, **78**, 2433 (1974).
(18) A. G. Urena, R. B. Bernstein, and G. R. Phillips, *J. Chem. Phys.*, **62**, 1818 (1975).
(19) W. N. Allen and F. W. Lampe, *J. Chem. Phys.*, **65**, 3378 (1976).
(20) W. N. Allen and F. W. Lampe, *J. Am. Chem. Soc.*, **99**, 2943 (1977).
(21) T-Y. Yu, T. M. H. Cheng, V. Kempter, and F. W. Lampe, *J. Phys. Chem.*, **76**, 3321 (1972).
(22) E. Teloy and D. Gerlich, *Chem. Phys.*, **4**, 417 (1974).
(23) G. Gloumousis and D. P. Stevenson, *J. Chem. Phys.*, **29**, 294 (1958).
(24) D. W. Setser, B. S. Rabinovitch, and J. W. Simons, *J. Chem. Phys.*, **40**, 1751 (1964).
(25) P. Potzinger, A. Ritter, and J. R. Krause, *Z. Naturforsch.*, **30a**, 347 (1975).
(26) L. Pauling, "The Nature of the Chemical Bond", Cornell University Press, Ithaca, N.Y., 1967, p 119.
(27) J. L. Franklin, J. G. Dillard, H. M. Rosentock, J. T. Herson, K. Drexl, and F. N. Field, *Nat. Stand. Ref. Data Ser., NSRDS-NBS*, 26 (1969).
(28) P. Potzinger and F. W. Lampe, *J. Phys. Chem.*, **74**, 719 (1970).
(29) F. P. Lossing and J. B. DeSousa, *J. Am. Chem. Soc.*, **81**, 281 (1959).
(30) K. M. Mackey and R. Watt, *Spectrochim. Acta*, **23a**, 2761 (1967).
(31) J. C. Hassler and D. W. Setser, *J. Chem. Phys.*, **45**, 3246 (1966).
(32) M. L. Vestal, *J. Chem. Phys.*, **43**, 1356 (1965).
(33) G. Z. Whitten and B. S. Rabinovitch, *J. Chem. Phys.*, **38**, 2466 (1963).
(34) Reference 16, pp 213, 216.
(35) I. M. T. Davidson, M. R. Jones, and C. Pett, *J. Chem. Soc.*, 937 (1967).

Potential Energy Surfaces for Some $C_4H_9O^+$ Ions; Rate-Determining Isomerizations Prior to Unimolecular Decompositions

Richard D. Bowen and Dudley H. Williams*

Contribution from the University Chemical Laboratory, Cambridge, CB2 1EW, United Kingdom. *Received April 15, 1977*

Abstract: A self-consistent explanation of the main reactions undergone in metastable transitions by some isomers of the $C_4H_9O^+$ ion is given in terms of the potential energy surfaces over which the reactions are considered to occur. It is shown that for some starting structures of $C_4H_9O^+$ the rate-determining step for dissociation is isomerization to another structure of $C_4H_9O^+$. The approach not only provides a simple explanation of the known chemistry, including isotopic labeling results, but also permits correct predictions to be made concerning the relative widths of the metastable peaks for the observed reactions, starting from different precursors.

In previous work,[1,2] we have shown that rate-determining isomerizations occur in the $C_3H_7O^+$ ion system prior to unimolecular decomposition. In particular, protonated acetone (**1**) was shown to undergo rate-determining rearrangement to protonated propionaldehyde (**2**), and the oxonium ion **3** to undergo rate-determining rearrangement to **4**, before dissociations (metastable transitions) occur.

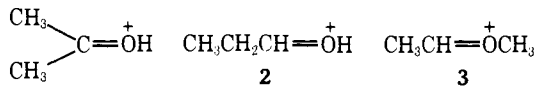

1 **2** **3**

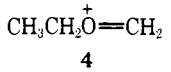

4

Although studies of $C_3H_7O^+$ are relatively numerous,[1-6] the higher homologue, $C_4H_9O^+$, appears to have received scant attention and it therefore seemed of interest to attempt to extend the approach used for $C_3H_7O^+$ to this ion. The metastable abundance data for the dissociation of the various ion structures possible for this ion, in which the charge may be considered as residing mainly on oxygen (i.e., the eight possible "onium" type ions) have already been documented.[7] The present work concerns four such structures, all of which may be conveniently generated in the gas phase by the fragmentation of suitable ethers, and the relevant data are summarized in Table I.

If the ions **5**–**8** are considered as higher homologues of the $C_3H_7O^+$ ions already investigated, it becomes apparent that **5** and **6** are both homologues of **4** which is known to undergo competitive loss of H_2O and C_2H_4 in metastable transitions. Further, the activation energies for these two processes are different[1] and are less than the energy (~40 kcal mol^{-1}) needed to produce $C_2H_5^+$ together with $CH_2{=}O$. In particular, loss of water from this ion, which must necessarily be a very complex reaction, dominates and requires only about 28 kcal mol^{-1} of internal energy.[1] Thus, the ions **5** and **6** would be expected to lose water with roughly the same activation energy as **4** unless another reaction can compete by virtue of possessing a similar activation energy.[8] Such a possibility could in principle arise by loss of ethylene (as occurs in the lower homolog **4**) or by loss of formaldehyde. The latter is observed to occur, with $CH_2{=}O$ loss accounting for about 15% of the metastable ion current for decomposition of **5** and **6**. The occurrence of formaldehyde loss is presumably due to the possibility of forming a secondary cation by direct bond cleavage of **6** (or bond cleavage with an associated 1,2-hydride shift in